

depression [30] anti-hyperglycemic [31] and antimicrobial [32-34] agent in plant extracts candidate them for overcoming more health problems. Thymus plant leaves and flower parts has good talent to applied for tonic and herbal tea, antiseptic, antitussive and carminative as well as treating cold [35-37]. Thymus oil and extracts applied in pharmaceutical, cosmetic and perfume industry besides flavoring and food preservation [38]. *Silybum marianum* cancer chemoprevention and hepatoprotection has high and brilliant role in treatment on of Phenolic compounds in aromatic extract and plants are one of the defensive mechanisms against bacterial agents, herbivore and insects [39-46]. Plants metabolites and/or constituent such as tannins, terpenoids, alkaloids, flavonoids, glycosides has more potential to be antimicrobial agent [47-50] and always the antimicrobial property of medicinal extract plants in presence and without of natural silver nanoparticles are significantly differ. In this research, *T. daenensis* and *S. marianum* absence of extracts combination with silver nanoparticles (Ag-NPs) in this media extensively was prepared and subsequently, used against some pathogenic bacteria and fungi to detect new sources of antimicrobial agents.

Materials and Methods

Chemicals, reagents and plant source

All reagents were of analytical grade and obtained from Merck, Dermasdat, Germany. The fresh and healthy plants of *T. daenensis*, *S. marianum* and *R. officinalis* were collected in June year 2013 from various areas of Yasouj district, Iran and subsequently were identified in photochemistry Lab in Yasouj University.

Extraction

Ultrasound-Assisted Extraction (UAE): Medicinal plants (*Thymus daenensis* and *Silybum marianum*) firstly washed thoroughly to remove impurities, shade dried and then ground to fine powder. Five grams (5.0 g) of Medicinal plants powder were placed in a copper tube and mixed with ethanol. The extraction process was performed with the ultrasonic device (JAC Ultrasonic 2010P, Jinwoo Engineering Co., Ltd., Hwasung, Gyeonggi, Korea) equipped with a digital timer and a temperature controller, the solvent used in the extraction was ethanol solution. The device was operated at a frequency of 40 kHz, an ultrasonic input power of 250 W. After ultrasonic extraction, the sample was centrifuged at 4000 rpm for 15 min, and the supernatant was collected. When the ultrasonic extraction was completed, the extracts were immediately cooled on ice to room temperature, filtered using a 5-mL syringe fitted with a 0.45 μm cellulose syringe filter (Phenomenex Australia Pty. Ltd., Lane Cove, Australia). Ultrasonication is a branch of acoustics that can be applied to solids, liquids and gases at frequencies above the human hearing range [51]. Ultrasonication generates an enormous interfacial area between the oil and alcohol due to micro turbulence leading to the formation of fine emulsions [52].

Preparation of *Rosmarinus officinalis* extract for synthesis of Ag-NPs

R. officinalis leaves were collected, chopped and dried for two days at room temperature. Dried leaves were washed thoroughly with distilled water and aqueous extract was prepared. Prepared extract was centrifuged and filtered through Whatman 41 filter paper to obtain clear solution. The filtrate was used immediately for Ag-NPs synthesis

which served as reducing and stabilizing agent. 50 mL of 1 mM AgNO_3 was added to 25 mL of aqueous extract of *R. officinalis* and mixed thoroughly via magnetic stirrer. The reaction mixture was then shaken to mixed completely and allowed to settle at room temperature. The color change to yellow confirm the formation of silver nanoparticles.

Purification of Ag-NPs

To separate unreacted components of reaction mixture was removed from the synthesized Ag-NPs the mixture was centrifuged [53] at 10000 rpm for 25 min and washed for three times using deionized water. Dried powder of the silver nanoparticles was obtained by freeze-drying. Ultra-centrifugation techniques were used to separated nanoparticles based on their size. Apart from centrifugation, chromatographic based separations such as HPLC and ion exchange chromatography was also utilized for separating nanoparticles from reaction mixture [54]. Separation of nanoparticle is a vital step in synthesis of nanoparticles from its reaction [55].

Characterization of synthesized nanoparticles

UV-Vis spectrometer (Perkin Elmer Lambda 25) was used to record absorbance in the range of 200-800 nm and also monitor the rate of Ag-NPs formation. 250 mL of each sample was diluted with 2 mL deionized water and sonicated for 15 min. The pH of stock solution (1 mg L^{-1}) was adjusted to 11.0 before scanning in quartz cuvettes with deionized water as reference. Factors such as temperature, pH, concentration of leaf extracts and concentration of AgNO_3 influences on the formation of Ag-NPs in the reaction mixture were examined by UV-Vis absorbance spectroscopy. The UV-Vis spectra of Ag-NPs which at RT dispersed in distilled water via 30 min of sonication and subsequently centrifuged at speed of 9000 rpm for 30 min was recorded. The pure Ag-NPs was prepared following removal of unbound ligand. X-ray diffraction (XRD) spectra were obtained by an automated Philips X'Pert X-ray diffractometer with Cu Radiation (40 kV and 30 mA) for 2θ values over range of 30°C-80°C. Scanning electron microscope (SEM: Hitachi S-4160) under an acceleration voltage of 30 kV. TEM analysis was recorded using TEM JEOL at 300 kV.

Biological activity

Antimicrobial assays: The well-diffusion method was used to study the antibacterial activity. All the glassware, media, and reagents used were sterilized in an autoclave at 121°C, 103 kPa of pressure for 21 min. *Staphylococcus aureus* (ATCC 25293), *Escherichia coli* (ATCC 33218) were used as model test strains for Gram-positive and Gram-negative bacteria, respectively. All the microbial cultures were adjusted to 0.5 McFarland standard, which are visually comparable to a microbial suspension of approximately 1.5×10^8 CFU/mL [56]. 100 μL of fresh bacterial culture was gently spread on the agar surface [57]. The bacterial concentration utilized was of 1.5×10^8 CFU/mL. 6 mm diameter filter paper disc, impregnated with 20 mL dose of each compounds. Using sterile disc (6 mm diameter) were bored into the seeded agar plates and these were loaded with 50 mL volume with concentration of 50, 25 and 12.5 mg L^{-1} of each compound reconstituted in dimethyl sulfoxide (DMSO). All the plates were incubated at 37°C for 24 h. Antibacterial activity of all the complexes was evaluated by measuring the diameter of zone of inhibition in mm (Table 1) and all investigation were undertaken using dimethyl sulfoxide (DMSO) as solvent. Amoxicillin, Cephalexin and Penicillin was used as controlled antibacterial agents and their results for

antibacterial activity was compared with under study material in Table 2.

Compound	Gram-positive			Gram-negative		
	S. aureus			E. coli		
	12.5	25	50	12.5	25	50
<i>T. daenensis</i>	14.00	15.70	17.62	13.40	15.00	15.22
<i>S. marianum</i>	9.70	10.50	12.30	8.50	10.10	11.38

<i>T. daenensis-Ag</i>	14.40	17.40	18.00	13.40	16.00	16.20
<i>S. marianum-Ag</i>	9.90	12.30	19.00	9.70	11.38	11.60
<i>S. marianum</i>	9.70	10.50	12.30	8.50	10.10	11.38

Table 1: Antibacterial activity of compounds in dose of (12.5, 25 and 50 mg L⁻¹). All tests were performed twice and all data are the mean of two measurements.

Antibiotic drugs	<i>Bacillus subtilis</i>	<i>Staphylococcus aureus</i>	<i>Pseudomonas aeruginosa</i>	<i>Escherichia coli</i>	<i>Candida albicans</i>	<i>Aspergillus oryzae</i>
Amphotericin B (0.03 mg/disc)	-	-	-	-	28.10	37.6
Amoxicillin (0.025 mg/disc)	28.10	41.60	-	20.80	-	-
Penicillin (0.01 mg/disc)	30.50	47.60	-	9.70	-	-
Cephalexin (0.03 mg/disc)	37.60	41.60	-	22.56	-	-

Table 2: Diameter of zone of inhibition (mm) of antibiotic drugs.

Antifungal screening by disc diffusion method: *Aspergillus oryzae* (PTCC 5164, *A. oryzae*) and *Candida albicans* (ATCC 10231, *C. albicans*) were used as mode for determinations of anti-fungal activities of extracts of *S. marianum* and *T. daenensis* by the disc diffusion method on the surface of Sabouraud Dextrose Agar inoculated with 1.0 10⁵ (CFU/mL) of spore suspension of fungi. The petri plates cultured with *Aspergillus oryzae* were incubated at 30°C for 24-48 h while the plates cultured with *C. albicans* were incubated at 32°C for 24-48 h. The discs impregnated with compounds solution (solubilized in 5% w/v DMSO) of compounds doses (12.5, 25 and 50 mg/disc) were dispensed at different positions on the agar plate [57]. At end of incubation period, antifungal activities of extracts were determined in term of inhibition zone diameter value. Antifungal activities of control drug Amphotericin B (0.03 mg/disc) is shown in Table 3.

Compound	<i>Candida albicans</i>			<i>Aspergillus oryzae</i>		
	12.5	25	50	12.5	25	50
<i>T. daenensis</i>	7.50	8.90	11.00	7.20	7.80	10.64
<i>S. marianum</i>	6.90	7.00	7.68	6.94	7.00	7.44
<i>T. daenensis-Ag</i>	8.12	9.38	11.20	8.00	8.10	10.70
<i>S. marianum-Ag</i>	7.20	7.50	8.12	7.10	7.22	7.68

Table 3: Antifungal activity of compounds in dose of (12.5, 25 and 50 µg L⁻¹). All tests were performed twice and all data are the mean of two measurements.

Determination of total phenolic content

The total phenolic content (TPC) of the *T. daenensis* and *S. marianum* extracts was determined by using the Folin-Ciocalteu reagent [58]. 100 µl of the diluted ethanolic extracts containing 500 µg

extract was mixed separately with (500 µl) Folin-Ciocalteu reagent and diluted with distilled water and 0.4 ml of (7.5% w/v) sodium carbonate solution (Na₂CO₃). The solution was mixed and allowed to stand for 1 hour at room temperature. Gallic acid solution (from 25 to 300 µg/ml) was used as a standard reagent. Finally, the absorbance was measured at 765 nm using a UV-Vis spectrophotometer. A calibration curve was prepared by using of standard solutions of gallic acid. The results were expressed as mg gallic acid equivalents (GAE)/gr of dried extract.

Determination of total flavonoid

Total flavonoid content of extracts was also determined [59]. 1 mg of extracts were diluted with 1000 µl of distilled water and 100 µl of 5% NaNO₂ solution were added. The mixture was kept at room temperature for 5 min and then, 200 µl of 10 % AlCl₃ were added to it. This mixture was incubated at room temperature for a 6 min then 1 ml of 1 M NaOH was added to the mixture. The solution absorbance at 510 nm was measured with a UV-Vis spectrophotometer. The concentration of the flavonoid compounds was calculated by using of the equation that obtained from the rutin (50-500 µg/ml) calibration curve.

Scavenging effect on 2, 2-diphenyl-1- picrylhydrazyl (DPPH)

Free radical scavenging activity was estimated by 2,2-diphenyl-1-picryl-hydrazyl (DPPH) assay by using of Von Gadow method with some modifications [60]. 2.4 ml of DPPH radical solution (24 µg/ml) prepared in 70% aqueous ethanol. The reaction mixture contained 100 µl of test extracts and 1 ml of methanolic solution of (24 µg/ml) of DPPH radical. The mixture was then shaken vigorously and incubated at 37°C for 10 min. The absorbance was measured at 517 nm by using by trolox solutions (100-1000 µg/ml) as a standard. Lower absorbance of the reaction mixture indicated higher free radical scavenging activity which was calculated using the following equation: DPPH scavenging effects (%) = 100 × (Ac-As)/(Ac) where Ac is the

absorbance of the control reaction and as is the absorbance of reaction mixture containing DPPH and extract at 517 nm.

FT-IR Spectrum analysis of extracts

FT-IR (JASCO FT/IR-460 System in the 400-4000 cm^{-1} , Japan) relies on the fact that the most molecules absorb light in the infra-red region of electromagnetic spectrum. This absorption corresponds specifically to the bonds present in the molecule. The frequency ranges are measured as wave numbers typically over the range 4000-400 cm^{-1} . Figure 1 shows the FT-IR peaks of dried extracts. Hydroxyl group in alcoholic and phenolic compound which is supported by the presence of a strong peak. The absorbance bands are associated with the stretch vibrations of alkyl C-C, conjugated C-C with a benzene ring, bending in plane of C-O-H, C-O stretch and bending out of plane C-H in saturated tertiary or secondary highly symmetric alcohol in extracts, respectively.

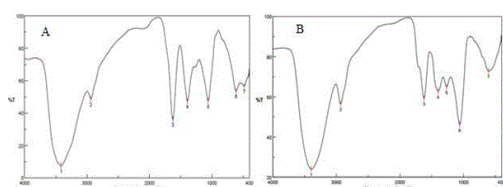


Figure 1: Fourier transform infrared absorption spectra of dried extracts. A) *T. daenensis* B) *S. marianum*.

Results and Discussion

Characterization of Ag-NPs

Figure 2 shows the FT-IR peaks of dried *R. officinalis* leaf extract. Typical peak of hydroxyl groups of phenolic compounds indicated by at 3397 cm^{-1} . The peaks at 2933 cm^{-1} , 1621 cm^{-1} , 1400 cm^{-1} , 1265 cm^{-1} , 1060 cm^{-1} and 605 cm^{-1} are associated with stretching vibrations of alkyl C-C, conjugated C-C of benzenoid rings, bending in plane of C-O-H, C-O stretch and bending out of plane C-H, respectively of saturated, tertiary and secondary symmetric hydroxylic groups of *R. officinalis* leaf extract.

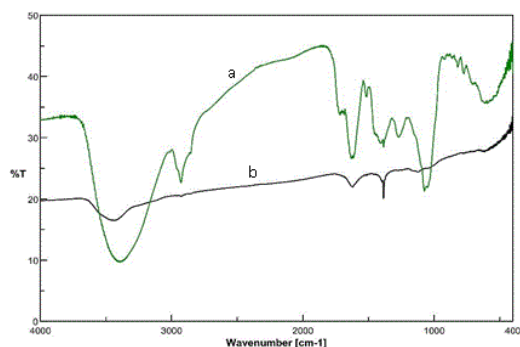


Figure 2: FT-IR spectra of (a) dried Rosmarinus officinalis leaf extract and (b) synthesized Ag-NPs.

The XRD pattern of Ag-NPs Figure 3a represent distinguished diffraction peaks at 2θ of 38.5° (111), 44.1° (200), 64.5° (2 2 0) and 77.3° (311) which strongly indicates the face-centered cubic (FCC) crystalline structure of Ag-NPs. According to Debye sheerer and half width of XRD patterns, average particle size of Ag-NPs was calculated around 33 nm and intense reflection at (111) compare to other peaks support the growth direction of nanocrystals. SEM image of drop-coated film of the Ag-NPs synthesized with *R. officinalis* leaf extract (Figure 3b) reveal spherical and uniformly nano-size Ag-NPs. TEM image (Figure 3c) also confirms the spherical shape of AgNPs which are of FCC oriented with aggregation, while its size range of 10-33 nm and average value is around 29 nm with good agreement with XRD data.

Reduction of Ag^+ ions to Ag (in 1 mM solution of AgNO_3) was traced by *R. officinalis* leaf extract absorption spectra as function of time reveal. (Figure 4a) shows the clear solution of *R. officinalis* leaf extract and Figure 4b shows the yellowish brown coloured Ag-NP's colloidal solution. Maximum absorbance was observed at 450 nm which is related to formation of Ag-NPs (Figure 3d) reveal that Plasmon resonance (SPR) of conducting electrons of Ag-NPs. This unique peak is due to surface *R. officinalis*. The nucleation process is acceleration slowly and reaction took about 4.5 h to complete, while no significant Ag-NPs formation was seen at 30 min. The rate of formation increases rapidly toward $t=270$ min and confirmed by adsorption platue at further time. The Ag-NPs synthesis was completed in 4.5 h and was very stable during further experiments. The XRD analysis was used to study the crystalline nature of green synthesized Ag-NPs.

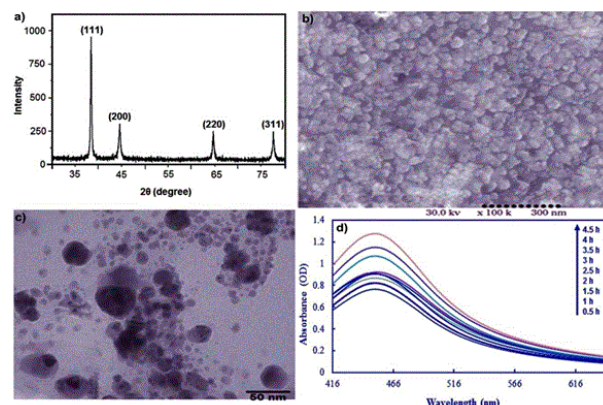


Figure 3: a) XRD pattern of green-synthesized silver nanoparticles by using leaf of *R.officinalis*, b) SEM image of Ag nanoparticles formed by *R.officinalis*, c) TEM image and d) Ultraviolet-visible spectra for formation of Ag-NP are as a function of time.

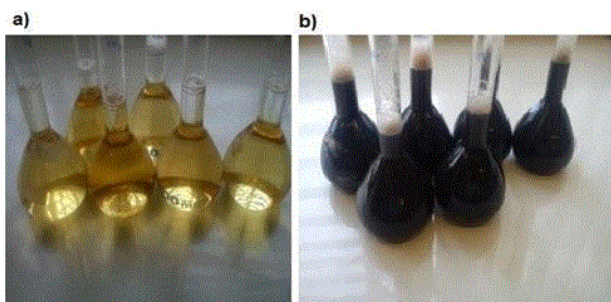


Figure 4: (a) Clear solution of *R.officinalis* leaf extract, (b) Ag-NP's after reaction of AgNO₃ with *R.officinalis* leaf extract.

Biological activity

Antimicrobial assays (*in vitro*): The *in vitro* antibacterial activity of Ag-NPs/extracts and *T. daenensis* and *S. marianum* extracts were evaluated based on the growth inhibition zone [mm; Figures 5-13; Tables 1-3]. Maximum zone of inhibition in concentrations (12.5, 25 and 50 mg/disc) was found to be (14.40, 17.4, 19) mm in *Staphylococcus aureus* (Table 1). The images of zone of inhibition in discs are shown in Figure 14. The solvent used for the preparation of compound solutions (DMSO) did not show inhibition against the tested organisms [as a negative control]. Extracts of *T. daenensis* and *S. marianum* exhibited significant activity against *S. aureus* and moderate activity against *E. coli* against. Finally, inhibitory effects of Ag-NPs/extracts confirm that the best effects and significant activity against *S. aureus* and *E. coli* even at low concentration [12.5 and 25 mg/mL]. Increasing the concentration of Ag-NPs /extracts solution to 50 mg/mL is associated with significant activity against *S. aureus* and *E. coli*, *Silybum-Ag* showed strong activity against *T. daenensis-Ag* at 50 mg/mL [Figures 6 and 3]. The Ag-NPs/ *T. daenensis* had the best effects and showed significant activity against pathogen bacteria even at low concentration [12.5-25 mg/mL] [Figures 5,6,8-11]. Compounds *T. daenensis*, *S. marianum* and Ag-NPs/extracts was active against *C. albicans* at 12.50, 25, 50 mg/mL concentration that have better antifungal activity against than *A.oryzae*, *T.daenensis* and Ag-NPs/ *Silybum*, better activity against *Silybum marianum* extract but was weak against Ag-NPs/ *Thymus* and *T.daenensis* extract [Figures 5-14].

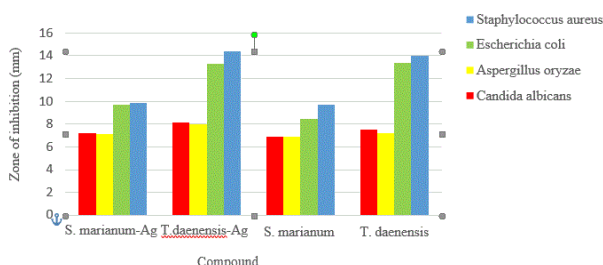


Figure 5: Antimicrobial activity of extracts in presence and without of Ag-NPs [12.5 mg/mL].

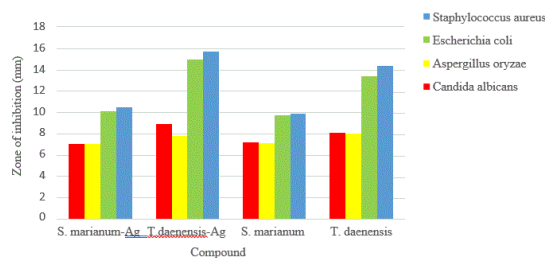


Figure 6: Antimicrobial activity of extracts in presence and without of Ag-NPs. [25 mg/mL].

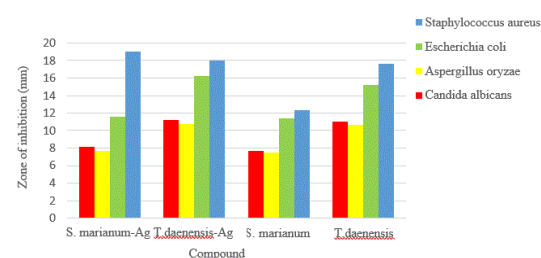


Figure 7: Antimicrobial activity of extracts in presence and without of Ag-NPs [50 mg/mL].

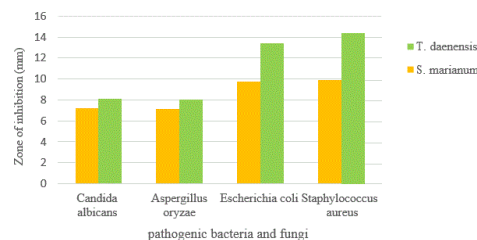


Figure 8: Antimicrobial activity of extracts in presence of natural silver nanoparticles [12.5 mg/mL].

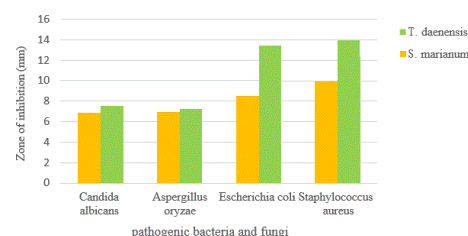


Figure 9: Antimicrobial activity of extracts [12.5 mg/mL].

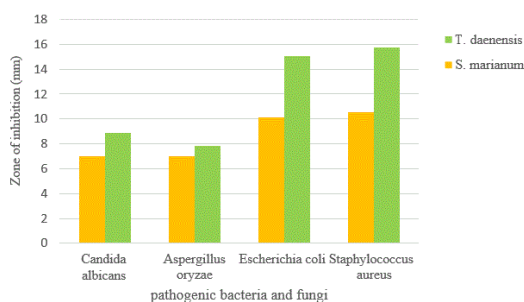


Figure 10: Antimicrobial activity of extracts [25 mg/mL].

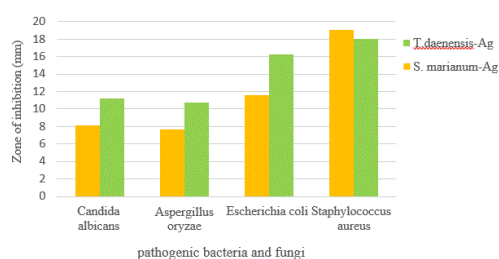


Figure 11: Antimicrobial activity of extracts in presence of natural silver nanoparticles [25 mg/mL].

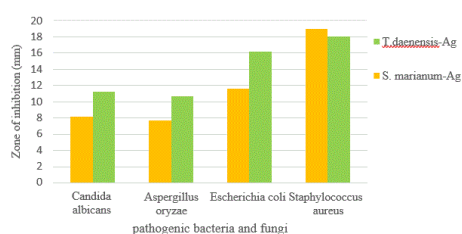


Figure 12: Antimicrobial activity of extracts [50 mg/mL].

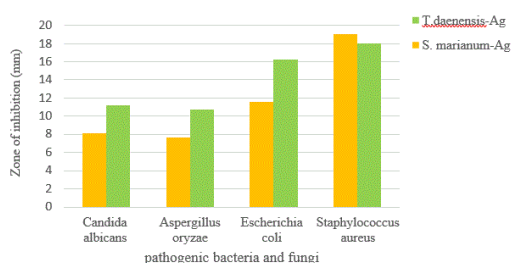


Figure 13: Antimicrobial activity of extracts in presence of natural silver nanoparticles [50 mg/mL].

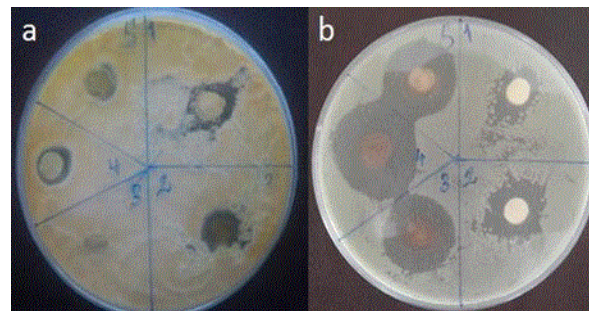


Figure 14: The inhibition halos for antifungal and (a) antibacterial activity (b) (50 mg L⁻¹).

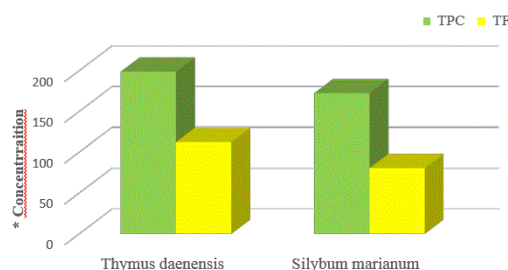


Figure 15: *TPC: mg gallic acid equivalent/g of dried extract and TF: mg rutin equivalents (RuE)/g of dried extract.

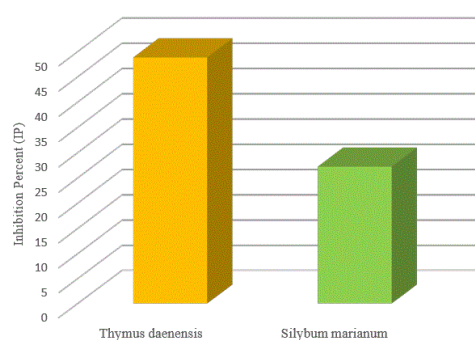


Figure 16: Comparison of inhibition percent.

Total flavonoids and phenolic content: Flavonoids are polyphenolic compounds which play an important role in stabilizing lipid oxidation and are also associated with antioxidative action [61]. Flavonoids found ubiquitously in plants and are the most common group of phytochemicals. Flavonoid content of the extracts in terms of (mg/g) rutin equivalents was recorded.

Phenols are the simplest bioactive phytochemicals having free radical scavenging ability due to the presence of hydroxyl groups. The sites and the numbers of hydroxyl groups are related to their relative toxicity for microorganisms, recently is shown that increasing in hydroxylation of these compounds cause to increasing in their toxicity properties [62]. The phenolic contents of hydroalcoholic extracts of

plants were tested using the diluted Folin-Ciocalteu reagent (FCR). Phenolic compounds react with FCR only under basic conditions (adjusted by a sodium carbonate solution to pH=10). Dissociation of a phenolic proton leads to a phenolate anion, which is capable of reducing FCR. The reaction occurs through electron transfer mechanism. The blue compounds formed between phenolate and FCR

are independent of the structure of phenolic compounds, therefore ruling out the possibility of coordination complexes formed between the metal center and the phenolic compounds. It is believed that FCR contains hetero polyphosphotunstates-molybdates [63]. The highest contents of total flavonoid and phenolics were observed for Shoot *L. usitatissimum* results clearly. (Table 4 and Figure 15).

Extracts	TPC ^a	TF ^b	(DPPH) inhibition %
<i>T. daenensis</i>	198.71 ± 1.50	172.42 ± 1.43	48.80 ± 0.59
<i>S. marianum</i>	112.44 ± 1.38	80.50 ± 1.41	27.20 ± 0.32

^aTPC: total phenolic content, mg gallic acid equivalent/g of dried extract

^bTF: total flavonoid content, mg rutin equivalents (RuE)/g of dried extract

Table 4: Total phenolic, flavonoid content and antioxidant activity of hydroalcoholic extracts.

Antioxidant capacity

Recently, using of antioxidants is proposed to protect people from oxidative stress damages. This study indicated that higher concentration of phenolic compounds in hydroalcoholic extracts improved antioxidant activity. Then these plants can be a use as a source of natural antioxidants to remove harmful effects of free radicals. The in-vitro antioxidant activity of test extracts were estimated by using of DPPH assay. DPPH radical-scavenging activity test measures the capacity of the extracts to scavenge the stable radical 2,2-diphenyl-1-picrylhydrazyl. If the extracts have this capacity, the initial blue/purple solution will change to a yellow color due to the formation of diphenyl picrylhydrazine. The antioxidants reacted with DPPH, a purple coloured stable free radical which accepts an electron or hydrogen radical to become a stable diamagnetic molecule. The amount of DPPH reduced was estimated by measuring the decrease in absorbance at 517 nm. The highest DPPH radical scavenging was obtained by aqueous/ethanolic extract of *T. daenensis* (Bois leaves 48.80 ± 0.59%) Figure 15 results was showed in Table 4. The different types of functional groups of extracts were identified from Figure 1 and Table 5.

S. No	Average Peaks value	Stretching	Interpretation
1	423.37	C-H bending outside of page	Alkanes
2	592.72	C-O Stretching	Alcohols
3	1067.22	O-H bending outside of page	Alcohols
4	1404.07	C-H Bending	Alkanes
5	1625.78	C=C Stretching	Alkenes
6	2932.12	C-H Stretching	Alkanes
7	3398.62	O-H Stretching	Alcohols

Table 5: Infrared spectrum analysis of extracts.

Conclusion

The antimicrobial activities of *T. daenensis* and *S. marianum* extracts and Ag-NPs/extracts assessed against pathogenic bacteria and fungi. Information of Tables of both samples was showed that

biological Ag nanoparticle (Ag-NPs/*T. daenensis* and Ag-NPs/*S. marianum*) has more antimicrobial effects to extracts (*T. daenensis* and *S. marianum*). Therefore, by completion of these experiments and the use of metal nanoparticles with plant extract in sensitive environments such as hospital, etc., suggested. Among the most promising nanomaterials with antibacterial properties are metallic nanoparticles, which exhibit increasing chemical activity due to their large surface to volume ratios and crystallographic surface structure. using of medicinal plant extracts with metal nanoparticles can be effective to eliminate the bacterial infections, as an alternative to antibiotics. *T. daenensis* and *S. marianum* are an abundant source of phenol and flavonoids, which have antioxidant properties and significantly reduce the effects of free radicals.

Acknowledgment

This work was supported by a grant from Research Council of Yasouj University.

References

- Egger S, Lehmann RP, Height MJ, Loessner MJ, Schuppler M (2009) Antimicrobial properties of a novel silver-silica nanocomposite material. Appl Environ Microbiol 75: 2973-2976.
- Bae E, Park HJ, Lee J, Kim Y, Yoon J, et al. (2010) Bacterial cytotoxicity of the silver nanoparticle related to physicochemical metrics and agglomeration properties. Environ Toxicol Chem 29: 2154-2160.
- Gurunathan S, Kalishwaralal K, Vaidyanathan R, Venkataraman D, Pandian SR, et al. (2009) Biosynthesis, purification and characterization of silver nanoparticles using Escherichia coli. Coll Surf B: Biointer 74: 328-335.
- Pal S, Tak YK, Song JM (2007) Does the antibacterial activity of silver nanoparticles depend on the shape of the nanoparticle? A study of the gram-negative bacterium Escherichia coli. Appl Environ Microbiol 73: 1712-1720.
- Chen W, Cai W, Zhang L, Wang G, Zhang L, et al. (2001) Sonochemical processes and formation of gold nanoparticles within pores of mesoporous silica. J Coll Interf Sci 238: 291-295.
- Ramajo L, Parra R, Reboredo M, Castro M (2009) Preparation of amine coated silver nanoparticles using triethylenetetramine. J Chem Sci 121: 83-87.
- Taubner T, Hillenbrand R (2005) Nanoscale-resolved subsurface imaging by scattering-type near-field optical microscopy. Optics Exp 13: 8893-8899.

8. Zhang L, RadovicMoreno AF, Alexis F, Gu FX, Basto PA, et al. (2007) Codelivery of hydrophobic and hydrophilic drugs from nanoparticle-aptamer bioconjugates. *Chem Med Chem* 2: 1268-1271.
9. Wiley B, Sun Y, Xia Y (2007) Synthesis of silver nanostructures with controlled shapes and properties. *Acc Chem Res* 40: 1067-1076.
10. Dwivedi P, Narvi SS, Tewari RP (2012) Green route to a novel Ag/PLGA bionanocomposite: A self-sterilizing surgical suture biomaterial. *Int J Adv Eng Sci Technol* 2: 236-243.
11. Shahverdi AR, Fakhimi A, Shahverdi HR, Minaian S (2007) Synthesis and effect of silver nanoparticles on the antibacterial activity of different antibiotics against *Staphylococcus aureus* and *Escherichia coli*. *Nanomedicine: Nanotechn Biol Med* 3: 168-1671.
12. Fayaz AM, Balaji K, Girilal M, Yadav R, Kalaichelvan PT, et al. (2010) Biogenic synthesis of silver nanoparticles and their synergistic effect with antibiotics: a study against gram-positive and gram-negative bacteria. *Nanomedicine: Nanotechn Biol Med* 6: 103-109.
13. Lara HH, Garza-Treviño EN, Ixtapan-Turrent L, Singh DK (2011) Silver nanoparticles are broad-spectrum bactericidal and virucidal compounds. *J Nanobiotech* 9: 30.
14. Illingworth B, Bianco RW, Weisberg S (2000) In vivo efficacy of silver-coated fabric against *Staphylococcus epidermidis*. *J Heart Valve Dis* 9: 135-1341.
15. Hoffmann S (1984) Silver sulfadiazine: an antibacterial agent for topical use in burns. *Scandinavian J Plastic Reconstr Surg* 18: 119-126.
16. Lara HH, Ayala-Núñez NV, Ixtapan-Turrent L, Rodríguez-Padilla C (2010) Mode of antiviral action of silver nanoparticles against HIV-1. *J Nanobiotechn* 8: 1.
17. Petrus EM, Tinakumari S, Chai LC, Ubong A, Tunung R, et al. (2011) A study on the minimum inhibitory concentration and minimum bactericidal concentration of Nano Colloidal Silver on food-borne pathogens. *Intern Food Res J* 18: 15-60.
18. Saito K, Uemura E, Ishizaki A, Kataoka H (2010) Determination of perfluorooctanoic acid and perfluorooctane sulfonate by automated in-tube solid-phase microextraction coupled with liquid chromatography-mass spectrometry. *Analytica chimica acta* 658: 141-146.
19. Prakash A, Sharma S, Ahmad N, Ghosh A, Sinha P (2011) Synthesis of AgNps By *Bacillus cereus* bacteria and their antimicrobial potential. *J Biomat Nanobiotech* 2: 156.
20. Bjerrum L, Munck A, Gahrn-Hansen B, Hansen MP, Jarbol DE, et al. (2011) Health Alliance for prudent antibiotic prescribing in patients with respiratory tract infections (HAPPY AUDIT)-impact of a non-randomised multifaceted intervention programme. *BMC Fam Pract* 12: 52.
21. Premanath R, Lakshmi Devi N (2010) Studies on Anti-oxidant activity of *Tinospora cordifolia* (Miers.) Leaves using in vitro models. *J Amer Sci* 6: 10.
22. KarabayYavasoglu NU, Sukatar A, Ozdemir G, Horzum Z (2007) Antimicrobial activity of volatile components and various extracts of the red alga *Jania rubens*. *Phytotherapy Res* 21: 153-156.
23. Mayer AM, Rodríguez AD, Berlinck RG, Hamann MT (2009) Marine pharmacology in 2005-2006: Marine compounds with anthelmintic, antibacterial, anticoagulant, antifungal, anti-inflammatory, antimalarial, antiprotozoal, antituberculosis, and antiviral activities; affecting the cardiovascular, immune and nervous systems, and other miscellaneous mechanisms of action. *Biochimica et Biophysica Acta (BBA)-General Subjects* 1790: 283-308.
24. Wang H, Provan GJ, Helliwell K (2004) Determination of rosmarinic acid and caffeic acid in aromatic herbs by HPLC. *Food Chem* 87: 307-311.
25. Vieira A (2010) A comparison of traditional anti-inflammation and anti-infection medicinal plants with current evidence from biomedical research: Results from a regional study. *Pharmacog Res* 2: 293.
26. Hajimehdipour H, Shekarchi M, Khanavi M, Adib N, Amri M (2010) A validated high performance liquid chromatography method for the analysis of thymol and carvacrol in *Thymus vulgaris* L. volatile oil. *Pharmacog Mag* 6: 154.
27. Zheng W, Wang SY (2001) Antioxidant activity and phenolic compounds in selected herbs. *J Agricult Food chem* 49: 5165-5170.
28. Ross R (1999) Atherosclerosis-an inflammatory disease. *New England J Med* 340: 115-126.
29. Ito H, Miyazaki T, Ono M, Sakurai H (1998) Antiallergic activities of rabdosiin and its related compounds: chemical and biochemical evaluations. *Bioorg Medic Chem* 6: 1051-1056.
30. Takeda H, Tsuji M, Matsumiya T, Kubo M (2002) Identification of rosmarinic acid as a novel antidepressive substance in the leaves of *Perilla frutescens* Britton var. *acuta* Kudo (*Perillae Herba*). *Japanese J Psychopharmac* 22: 15-22.
31. Kumar PM, Sasmal D, Mazumder PM (2010) The antihyperglycemic effect of aerial parts of *Salvia splendens* (scarlet sage) in streptozotocin-induced diabetic-rats. *Pharmacog Res* 2: 190.
32. Jain R, Kosta S, Tiwari A (2010) Ayurveda and urinary tract infections. *J Young Pharmac* 2: 337.
33. Zomorodian K, Saharkhiz MJ, Rahimi MJ, Bandegi A, Shekarkhar G, et al, (2011) Chemical composition and antimicrobial activities of the essential oils from three ecotypes of *Zataria multiflora*. *Pharmacog Mag* 7: 53.
34. Ghorbani A (2005) Studies on pharmaceutical ethnobotany in the region of Turkmen Sahra, North of Iran:(Part 1): General results. *J Ethnopharmacol* 102: 58-68.
35. Djeridane A, Yousfi M, Nadjemi B, Boutassouna D, Stocker P, et al. (2006) Antioxidant activity of some Algerian medicinal plants extracts containing phenolic compounds. *Food chem* 97: 654-660.
36. Seyyednejad SM, Motamedi H (2010) A Review on native medicinal plants in Khuzestan, Iran with antibacterial properties. *Intern J pharmacol* 6: 551-560.
37. Bauer K, Garbe D, Surburg H (2008) Common fragrance and flavor materials: preparation, properties and uses. John Wiley and Sons.
38. Polyak SJ, Ferenci P, Pawlotsky JM (2013) Hepatoprotective and antiviral functions of silymarin components in hepatitis C virus infection. *Hepato* 57: 1262-1271.
39. Polyak SJ, Oberlies NH, Pécheur EI, Dahari H, Ferenci P, et al. (2013) Silymarin for hepatitis C virus infection. *Antiviral Therapy* 18: 141.
40. Abenavoli L, Capasso R, Milic N, Capasso F (2010) Milk thistle in liver diseases: past, present, future. *Phytother Res* 24: 1423-1432.
41. Agarwal R, Agarwal C, Ichikawa H, Singh RP, Aggarwal BB (2006) Anticancer potential of silymarin: from bench to bed side. *Anticancer Res* 26: 4457-4498.
42. Deep G, Agarwal R (2010) Antimetastatic efficacy of silibinin: molecular mechanisms and therapeutic potential against cancer. *Cancer Metast Rev* 29: 447-463.
43. Ramasamy K, Agarwal R (2008) Multitargeted therapy of cancer by silymarin. *Cancer Lett* 269: 352-362.
44. Comelli MC, Mengs U, Schneider C, Prosdociami M (2007) Toward the definition of the mechanism of action of silymarin: activities related to cellular protection from toxic damage induced by chemotherapy. *Integra Canc Therap* 6: 120-129.
45. Gazak R, Walterova D, Kren V (2007) Silybin and silymarin-new and emerging applications in medicine. *Curr Medic Chem* 14: 315-338.
46. Cowan MM (1999) Plant products as antimicrobial agents. *Clinic Microbiol Rev* 12: 564-582.
47. Dahanukar SA, Kulkarni RA, Rege NN (2000) Pharmacology of medicinal plants and natural products. *Indian J pharmacol* 32: 81-118.
48. Gul HI, Sahin F, Gul M, Ozturk S, Yerdelen KO (2005) Evaluation of antimicrobial activities of several Mannich bases and their derivatives. *Archiv der Pharmazie* 338: 335-338.
49. Ramasamy S, Manoharan AC (2004) Antibacterial effect of volatile components of selected medicinal plants against human pathogens. *Asian J Microbiol Biotech Environ Sci* 6: 209-210.
50. Ensminger D, Bond LJ (2011) Ultrasonics: fundamentals, technologies and applications. CRC press.

51. Choudhury HA, Chakma S, Moholkar VS (2014) Mechanistic insight into sonochemical biodiesel synthesis using heterogeneous base catalyst. Ultrason Sonochem 21: 169-181.
52. Brakke MK (1961) Density gradient centrifugation and its application to plant viruses. Adv Virus Res 7: 193-224.
53. Jimenez VL, Leopold MC, Mazzitelli C, Jorgenson JW, Murray RW (2003) HPLC of monolayer-protected gold nanoclusters. Anal Chem 75: 199-206.
54. Kowalczyk B, Lagzi I, Grzybowski BA (2011) Nanoseparations: strategies for size and/or shape-selective purification of nanoparticles. Current Opin Coll Interf Sci 16: 135-148.
55. Bauer AW, Kirby WM, Sherris JC, Turck M (1966) Antibiotic susceptibility testing by a standardized single disk method. Amer J Clin Pathol 45: 493.
56. Chohan ZH, Youssoufi MH, Jarrahpour A, Hadda TB (2010) Identification of antibacterial and antifungal pharmacophore sites for potent bacteria and fungi inhibition: Indolenyl sulfonamide derivatives. Europ J Medic Chem 45: 1189-1199.
57. McDonald S, Prenzler PD, Antolovich M, Robards K (2001) Phenolic content and antioxidant activity of olive extracts. Food Chem 73: 73-84.
58. Zhishen J, Mengcheng T, Jianming W (1999) The determination of flavonoid contents in mulberry and their scavenging effects on superoxide radicals. Food Chem 64: 555-559.
59. Von Gadow A, Joubert E, Hansmann CF (1997) Comparison of the antioxidant activity of aspalathin with that of other plant phenols of rooibos tea (*Aspalathus linearis*), α -tocopherol, BHT, and BHA. J Agric Food Chem 45: 632-638.
60. Xing GX, Li N, Wang T, Yao MY (2003) Advances in studies on flavonoids of licorice. China J Chinese Mat Med 28: 593-597.
61. Fujiki H, Yoshizawa S, Horiuchi T, Suganuma M, Yatsunami J, et al. (1992) Anticarcinogenic effects of (-)-epigallocatechin gallate. Prevent Med 21: 503-509.
62. Huang D, Ou B, Prior RL (2005) The chemistry behind antioxidant capacity assays. J Agric Food Chem 53: 1841-1856.
63. Yamaguchi T, Takamura H, Matoba T, Terao J (1998) HPLC method for evaluation of the free radical-scavenging activity of foods by using 1,1-diphenyl-2-picrylhydrazyl. Biosci Biotech Biochem 62: 1201-1204.